JOURNAL OF Materials Feature Article CHEMISTRY

A review of cation-ordered rock salt superstructure oxides

Glenn C. Mather,*†[a] Christian Dussarrat,[b] Jean Etourneau[b] and Anthony R. West[c]

[a]*Departamento de Engenharia Cerâmica e do Vidro, Universidade de Aveiro, 3810-193 Aveiro, Portugal*
[b]*Institut de chimie de la matière condensée de Bordeaux, Château Brivazac, Avenue du Dr. A. Schweitzer, 33600 Pessac, France*
[c]*University of Sheffield, Department of Engineering Materials, Sir Robert Hadfield Building, Mappin Street, Sheffield, UK S1 3JD*

Received 31st January 2000, Accepted 30th June 2000
First published as an Advanced Article on the web 15th August 2000

The types of structures formed when two or more cations occupy the sodium sites in the NaCl unit cell in a non-random manner are reviewed with reference to the cation arrangement in layers of close-packed octahedra and the cation arrangement in the NaCl subcell. Factors influencing the stability of particular structure types, including bond valence and radius ratios, are discussed.

Introduction

The NaCl or rock salt structure is one of the most common and well known structure types adopted by compounds of composition AX. The cation, A, is often either an alkali metal, alkaline earth or transition series cation and X is most commonly an oxide, sulfide or halide. The cations are octahedrally coordinated by anions, as are the anions by cations; in terms of a polyhedral structure description, both sets of counter-ions are distributed in a three-dimensional network of edge-sharing octahedra. The rock salt structure is unique in displaying regular octahedral coordination for both cations and anions.

Until a few years ago, known rock salt superstructure phases arose almost exclusively in materials containing two crystallographically distinct types of cation, occupying the sodium sites in a non-random manner. More recently, superstructure phases which display ordering among three cation sites have been synthesised. We consider it timely, therefore, to describe the ordered configurations which are observed and review the factors which influence which type of cation order is adopted. This review excludes substoichiometric phases, where the cation order is not one-to-one, and non-oxide phases, such as carbides.

General considerations

The sizes of the anions and cations in any structure place an upper and lower limit on their coordination environment and, thus, on the type of structure which is adopted. The sizes of ions which are appropriate for a particular structure may, to a first approximation, be determined by geometry and expressed by radius ratio rules. The NaCl structure often forms when small cations occupy octahedral vacancies between cubic close-packed (ccp) anion layers. Equally, small anions may occupy octahedral holes in a close-packed (cp) cation array. When the counter-ions are of similar size, either the NaCl structure or the CsCl structure may form. If the anions (or cations) are not as closely packed as possible (closest packed), then the structure is sometimes termed eutactic.[1,2] Many rock salt phases, such as BaO and SrO, are eutactic in nature, as are the rock salt-like layers in superconducting rock salt–perovskite intergrowth phases. In general, if atoms are assumed to be incompressible spheres, the NaCl structure is most favourable for a composition AX with cation radius r_A and anion radius r_X, constrained by the relation $0.42 \leqslant r_A/r_X \leqslant 0.72$.[3,4] If $r_A/r_X = 0.42$, the anion layers are closest-packed but for greater values, the structure formed is eutactic since the anions are not in contact. The above relationship applies equally well for the inverse ratio, r_X/r_A, in which the cations form a closest-packed array for $r_X/r_A = 0.42$. However, whilst radius ratio rules provide useful guidelines as a first approximation, the notion that radii are fixed is now widely discounted. Different, but self-consistent, tables of ionic radii are available and show, for instance, that the radius of a given ion varies with coordination number.

A rather useful concept is Pauling's rule of electroneutrality. This states that the sum of electrovalencies, z/n (z = charge, n = coordination no.) of the nearest neighbour cations should equal the charge, x, of the anion, *i.e.* $\Sigma z/n = x$. A modification to the electroneutrality rule, which takes account of differences in bond strengths and bond lengths in more complex structures, is the concept of bond valence.[4–9] The bond valence rule extends Pauling's electroneutrality rule to structures in which distortions occur or to structures in which the bonding cannot be considered as ionic. The electrostatic bond strength is replaced by a bond valence, b_{ij}, which is defined in a similar way to the electrostatic bond strength. Both the Pauling and bond valence concepts are useful in discussing and classifying ordered rock salt configurations.

In ternary rock salt oxide systems, $A_aB_bO_{a+b}$, the two cations, A and B, usually have different valence. However, there are only certain A, B combinations in which local electroneutrality around oxygen is preserved. These occur in the general formulae ABO_2, A_2BO_3 and A_5BO_6, for which A is monovalent and B is tri-, tetra- and heptavalent, respectively, as shown by the following:

ABO_2 has OA_3B_3 octahedra; $\sum z/n = (3 \times 1/6) + (3 \times 3/6) = 2$

A_2BO_3 has OA_4B_2 octahedra; $\sum z/n = (4 \times 1/6) + (2 \times 4/6) = 2$

A_5BO_6 has OA_5B octahedra; $\sum z/n = (5 \times 1/6) + (1 \times 7/6) = 2$

With other A,B combinations, specifically A_3BO_4 and A_4BO_5, although the structures as a whole are electroneutral, local electroneutrality around each oxygen cannot be satisfied,

†Current address: Netherlands Energy Research Foundation, ECN, P.O. Box 1, NL 1755 ZG, Petten, Netherlands. E-mail: mather@ecn.nl

since the total number of cations per formula unit is not a factor of six. The structures cannot be composed of octahedra in which the ratio of A to B coordinating cations is the same for every oxygen. We first consider those ordered rock salt structures in which Pauling's rule of electrovalence is satisfied, since most ordered rock salt structures belong in this category, and secondly, review some which do not not conform to Pauling's rule.

ABO_2

Almost all rock salt superstructures of formula ABO_2 are isostructural with β-$LiFeO_2$, γ-$LiFeO_2$ or α-$NaFeO_2$. In order to compare them, the A–B cation order is discussed, with reference to the cubic or pseudo-cubic rock salt subcell of each, in two ways. First, it is useful to consider the A and B cation arrangements in layers between the cp anion layers, *i.e.* parallel to {1 1 1}. However, whereas there are four equivalent orientations of such cation layers in the simple rock salt structure, in the various superstructures, the layer arrangements generally differ in the different orientations. Each case is considered in turn; usually the cation arrangement is simplest in one of the four orientations and this gives rise to the preferred description. Secondly, in the NaCl unit cell (Fig. 1) the cations lie in rows parallel to ⟨1 1 0⟩ at heights of $z=0$ and $z=0.5$. Different ordering sequences occur within these rows, and for the simpler ABO_2 structures, it is useful to compare these sequences.

γ-$LiFeO_2$

γ-$LiFeO_2$‡ is formed by heating metastable β-$LiFeO_2$ at 500 °C;[10] above 650 °C, Li and Fe disorder. The order adopted by Li and Fe between cp oxygen layers is shown in Fig. 2. In γ-$LiFeO_2$, the A and B cations order in the sequence ABAB parallel to both [1 1 0] and [−1 1 0] of the rock salt subcell (Fig. 3.) to give a tetragonal body-centered unit cell with a *c*-parameter which is double that of the NaCl subcell.[11]

Table 1 gives the crystallographic parameters of the ABO_2 structure types. The γ-$LiFeO_2$ superstructure is adopted by a large family of phases, including the compounds $LiMO_2$ (M = Sc, In),[12,13] $NaMO_2$ (M = Gd, Eu, Sm, Nd, Pr, La) and Li_2MXO_4 (M = Mg, Mn, Co, Zn; X = Zr, Hf),[14] in which the M and X cations are disordered over the Fe sites. The anatase (TiO_2) structure is related to that of the γ-$LiFeO_2$ structure type in that the Li site (4b) is unoccupied. $KSbS_2$ has a monoclinic distortion of the γ-$LiFeO_2$ structure.[15]

β-$LiFeO_2$

β-$LiFeO_2$ forms at 450 °C from disordered $LiFeO_2$, and is a precursor to the formation of stable γ-$LiFeO_2$. Initially, a body-centred unit cell was proposed for β-$LiFeO_2$,[10] but it was subsequently shown to be monoclinic.[16–22] Fig. 4 shows how Li and Fe order between cp oxygen layers. A and B order in the sequence ABBAAB parallel to [1 1 0] (Fig. 5), but ABAB parallel to [−1 1 0], as is the case for γ-$LiFeO_2$. This ordering pattern is adopted at both $z=0$ and $z=0.5$ of the subcell.

α-$NaFeO_2$

In the α-$NaFeO_2$ structure, cations order into alternate layers perpendicular to [1 1 1]; this structure is closely related to that of $CdCl_2$, in which layers of Cd and cation vacancies alternate perpendicular to [1 1 1].[22] Rows of like cations run parallel to [1 1 0] at heights of $z=0$, 0.5 (Fig. 6), but alternate ABAB parallel to [−1 1 0].

The layered nature of α-$NaFeO_2$ allows facile cation (de)intercalation and isostructural lithium oxides ($LiMO_2$: M = Co, Ni, V, Cr)[23] have been studied as potential cathode materials in solid-state lithium batteries. Recently, layered $LiMnO_2$ was synthesised using an ion-exchange technique.[24] The phase β-$NaNiO_2$ (space group *C*2/*c*) has a monoclinic distortion of α-$NaFeO_2$.[25]

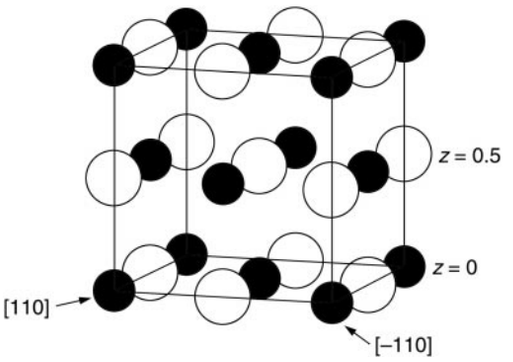

Fig. 1 NaCl unit cell. Anions and cations are shown as white spheres and black spheres, respectively.

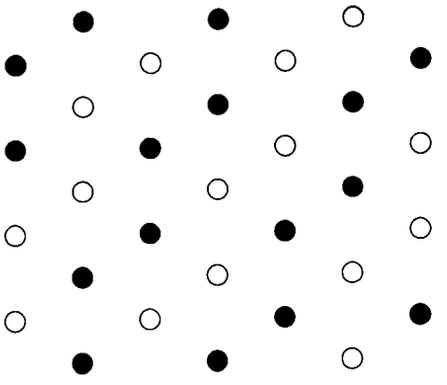

Fig. 2 Arrangement of Li and Fe cations between cp oxygen layers in γ-$LiFeO_2$. Li ions are shown as white circles and Fe ions as black circles.

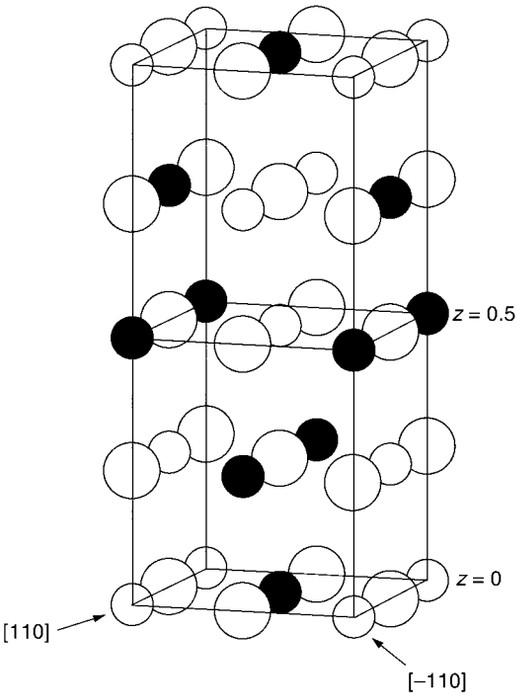

Fig. 3 Crystal structure of γ-$LiFeO_2$; NaCl subcell is outlined. Li ions are shown as small white spheres, Fe ions as small black spheres and oxygen ions as large white spheres.

‡Tetragonal $LiFeO_2$ is described here as γ-$LiFeO_2$, but is often referred to in the literature as α-$LiFeO_2$.

Table 1 Crystallographic data for ABO_2 rock salt superstructures

Atom	Position	x	y	z	Analogues
γ-$LiFeO_2$: $I4_1/amd$ ($Z=8$), $a=4.049$, $c=8.742$ Å					
Li	4b	0	0	1/2	$LiMO_2$ (M = Sc, In),
Fe	4a	0	0	0	$NaMO_2$ (M = Gd,
O	8e	0	0	1/4	Eu, Sm,Nd), Li_2MXO_4 (M = Mg, Mn, Co; X = Zr, Hf)
β-$LiFeO_2$: $C2/c$ ($Z=4$), $a=8.871$, $b=11.590$, $c=5.147$ Å, $\beta=145.70°$					
Li1	4e	0	9/16	1/4	None known
Li2	4e	0	13/16	1/4	
Fe1	4e	0	1/16	1/4	
Fe2	4e	0	5/16	1/4	
O1	8f	1/4	1/16	1/4	
O2	8f	1/4	5/16	1/4	
α-$NaFeO_2$: $R\bar{3}m$ ($Z=3$), $a=3.025$, $c=16.094$ Å					
Na	3a	0	0	0	$LiMO_2$ (M = Co,
Fe	3b	0	0	1/2	Mn, Ni. V, Cr)
O	6c	0	0	0.231	
$Li_2Ti_2O_4$: $Fd\bar{3}m$ ($Z=8$), $a=8.756$ Å					
L	16d	1/2	1/2	1/2	None known
Ti	16e	0	0	0	
O	32c	0.2552	0.2552	0.2552	

$Li_2Ti_2O_4$

$LiTiO_2$ adopts the NaCl structure with statistical cation disorder.[26,27] However, a second metastable polymorph can be synthesised by chemical lithiation of the spinel $LiTi_2O_4$.[28–30] The formation mechanism involves not only intercalation but a displacement of Li in $LiTi_2O_4$ from tetrahedral to octahedral sites. The structure of $Li_2Ti_2O_4$ is similar to that of α-$NaFeO_2$, but one quarter of the Li and Ti atoms have changed planes so that the alternate cation layers perpendicular to [1 1 1] are ¾Li, ¼Ti and *vice versa* (Fig. 6). The order adopted by the Li and Ti cations in consecutive layers between cp oxygens is shown in Fig. 7(a) and (b).

Comparison of ABO_2 structure types

Coordination environment of oxygen. In rock salt phases, ABO_2, which satisfy Pauling's rule of electroneutrality, only two ordered cation arrangements are possible in the first coordination shell of oxygen. These are termed *dispersed* and *clustered* and are shown in Fig. 8. In a dispersed arrangement, like cations are situated as far apart as possible, whereas in a clustered arrangement, they are as close together as possible. All the structures described so far are composed of either or both of these types of octahedra which edge-share in three dimensions. A dispersed arrangement is found in γ-$LiFeO_2$ and a clustered arrangement in α-$NaFeO_2$. The $Li_2Ti_2O_4$ arrangement is also clustered but differs from α-$NaFeO_2$ by the manner in which the octahedra are oriented relative to one another. In β-$LiFeO_2$, both clustered and dispersed arrangements are found.

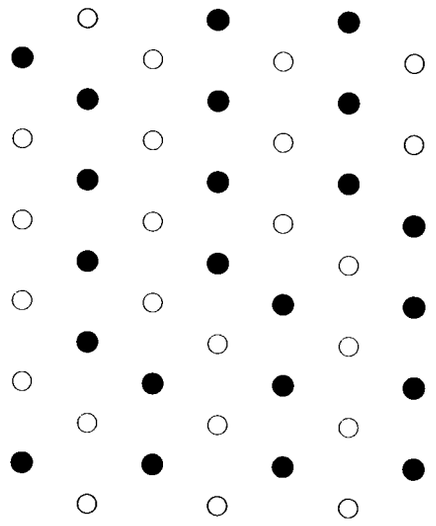

Fig. 4 Cation order between Li (white circles) and Fe (black circles) in β-$LiFeO_2$. These layers are perpendicular to the [2 4 −1] direction.

Relative stability of ABO_2 phases. Brunel *et al.* studied the factors which dictate the stability fields of ABO_2 rock salt phases.[31] From lattice energy considerations, with cations in ideal positions within the crystal lattice, the γ-$LiFeO_2$ structure with dispersed cation arrangement should be thermodynamically stable. However, the internal energy may be modified if there are different site size requirements for the A and B cations

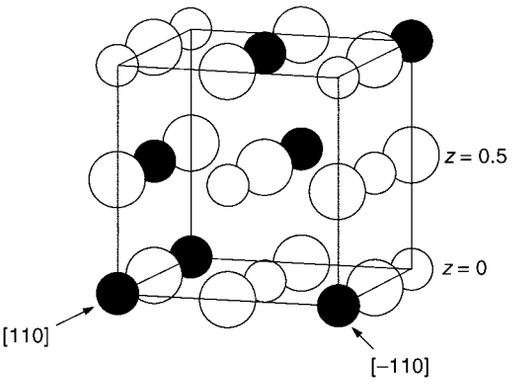

Fig. 5 NaCl subcell showing the cation order adopted in α-$LiFeO_2$. Li ions are shown as small white spheres, Fe ions as small black spheres and oxygen ions as large white spheres.

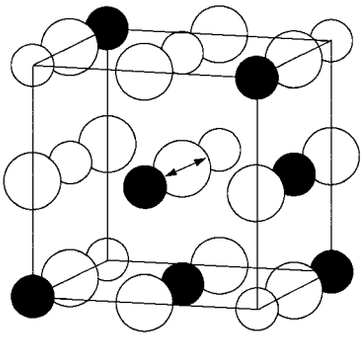

Fig. 6 NaCl subcell showing the cation order adopted in α-$NaFeO_2$. The cation order adopted in $Li_2Ti_2O_4$ is related to that in α-$NaFeO_2$ by the cation interchange indicated by the arrows. Na ions are shown as small white spheres, Fe ions as small black spheres and oxygen ions as large white spheres.

and if one or the other is particularly polarising towards oxygen. The energy associated with cation order alone favours the γ-$LiFeO_2$ structure type (dispersed arrangement) since the more highly charged [Fe(III)] cations are as far apart as possible; Coulombic repulsion terms are, thus, minimised. However, the anions are much more polarized in a clustered arrangement, since oxygen can be displaced towards all three trivalent cations, so a structure with this environment is preferred when small highly polarizing B^{3+} cations are present. In such structures, the polarisation energy of the anions is an important factor in the crystal lattice energy. Conversely, when the trivalent cations are too large, a dispersed environment becomes favourable. In this cation arrangement, oxygen can only be displaced towards a single trivalent cation such as is found in the γ-$LiFeO_2$ structure type. Thus, as a general guideline, we can say that the structure adopted is simply a function of the corresponding trivalent to monovalent cation radius ratio (r_B/r_A).

In another investigation into the stability of ordered rock salt phases, reported by Hauck,[32] the discussion extends to A_2BO_3 and A_5BO_6 systems. This work concludes that stable superstructures form as a result of Coulombic repulsion between the highly charged B cations: B–B cation distances are maximized and B–B cation repulsion energies minimized, with a consequent reduction in volume per formula unit compared to the disordered dimorph of the same composition.

A_2BO_3

In A_2BO_3 phases, there are again two types of octahedra, shown in Fig. 9, which satisfy the electroneutrality condition. The tetravalent B cations are either *cis* (clustered) or *trans* (dispersed) within the OA_4B_2 octahedra. The superstructures which form by edge-sharing of the AO_6, BO_6 octahedra are most simply compared if we consider the relationship amongst the BO_6 octahedra, and also how A and B order between the cp oxygen layers.

β-Li_2SnO_3

Li_2SnO_3 displays two structures, both of which are related to α-$NaFeO_2$, but contain a layer of Li which alternates with a layer of one third Li and two thirds Sn, such that the formula may be written as $Li(Li_{1/3}Sn_{2/3})O_2$. The high-temperature rhombohedral form, α-Li_2SnO_3, shows a statistical distribution of Li,Sn within the mixed cation layer and is isostructural with α-$NaFeO_2$. The low-temperature polymorph, isostructural with Li_2TiO_3,[33] has Li–Sn order within the mixed cation layer and its symmetry is reduced from rhombohedral to monoclinic.[34] Crystallographic parameters for β-Li_2SnO_3 and the other

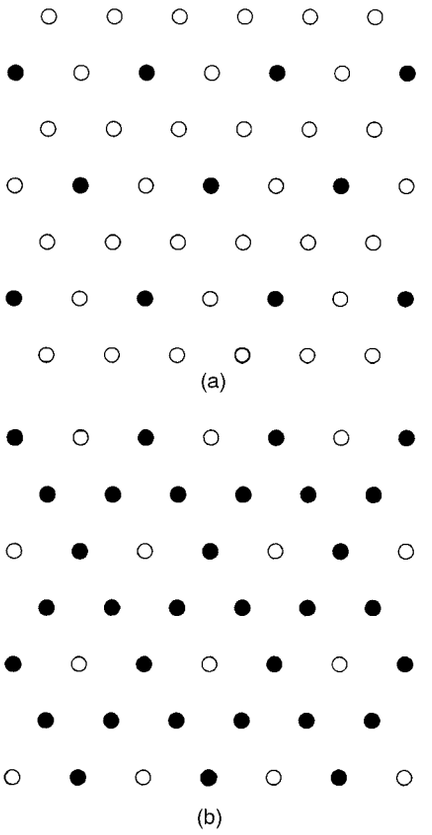

Fig. 7 Order adopted by Li (white circles) and Ti (black circles) in consecutive layers between cp oxygens in $Li_2Ti_2O_4$.

A_2BO_3 structure types are given in Table 2. The OLi_4Sn_2 octahedra have the Sn atoms in a *cis* configuration (Fig. 9). Within the mixed cation layer, SnO_6 octahedra edge-share with

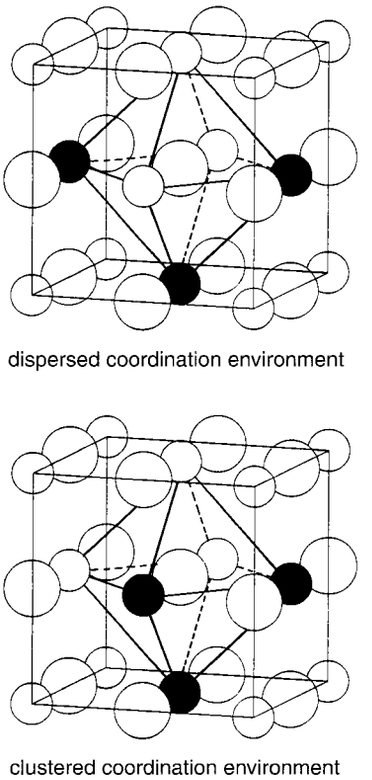

Fig. 8 Octahedral cation arrangements in ABO_2 rock salt phases. A cations are shown as small white spheres, B cations as small black spheres and O anions as large white spheres.

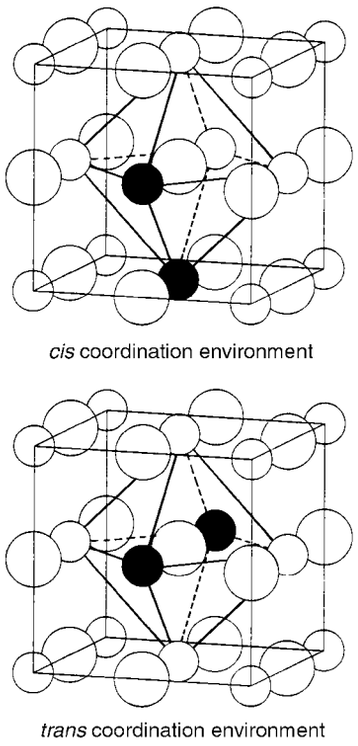

Fig. 9 Octahedral cation arrangements in A_2BO_3 rock salt phases. A cations are shown as small white spheres, B cations as small black spheres and O anions as large white spheres.

three other SnO_6 octahedra [Fig. 10(a)]. The Sn–Li arrangement within the mixed layers [Fig. 11(a)] is identical to that of Li and Ti in alternate cation layers of $Li_2Ti_2O_4$.

Li_2ZrO_3

Li_2ZrO_3 occurs in two forms. One has a partially ordered structure, isostructural with γ-$LiFeO_2$, in which the iron sites are occupied by two thirds Zr and one third Li.[35] The fully ordered, monoclinic, low-temperature form has entirely mixed layers of Li, Zr and alternate layers are staggered,[36] Fig. 11(b). Within each mixed cation layer, ZrO_6 octahedra edge-share with two other ZrO_6 octahedra to form chains; between the layers, ZrO_6 octahedra corner-share giving an open, 3D network of ZrO_6 octahedra, Fig. 10(b). Both *cis* and *trans* Zr configurations occur.

β-Na_2PtO_3

Na_2PtO_3 forms two ordered rock salt structures. α-Na_2PtO_3 is isostructural with β-Li_2SnO_3; low-temperature β-Na_2PtO_3 has mixed cation layers as in Li_2ZrO_3, but a different cation ordering pattern is observed, Fig. 11(c).[37] The cation layers are staggered to form a six-layer repeat sequence. Fig. 10(c) shows the arrangement adopted by the PtO_6 octahedra within the unit cell. Each PtO_6 octahedron shares with another within a layer and also edge-shares with a PtO_6 octahedron in the layers above and below.

Comparison of A_2BO_3 structure types

In β-Li_2SnO_3, the Sn cations lie in Li–Sn layers which alternate with layers of Li. Oxygen may, thus, become more easily polarized in the same manner as in α-$NaFeO_2$. The polarization energy of the oxygens, associated with the tetravalent cations lying in the same layer, would, therefore, appear to be greater than the energy gained by maximizing B–B cation distances. In Li_2ZrO_3, each cation layer is mixed; the tetravalent cations are situated both *cis* and *trans* to each other so, on average, there is a greater B–B cation distance. The energy gain associated with maximizing the B–B cation distance would, thus, appear to be dominant in this case. As Zr^{4+} is slightly larger than Sn^{4+}, we may presume that, as in ABO_2 systems, the choice of structure adopted is a function of the size and, consequently, polarizing power of the B cations. The β-Na_2PtO_3 structure shows only edge-sharing BO_6 octahedra which are found in each cation layer. The structure would appear, therefore, to be intermediate between the β-Li_2SnO_3 and Li_2ZrO_3 structure types. The structures of β-Li_2SnO_3 and β-Na_2PtO_3 are related in a similar manner to the way in which the α-$NaFeO_2$ structure is related to the $Li_2Ti_2O_4$ structure type in ABO_2 systems. Both structures are

Table 2 Crystallographic data for A_2BO_3 rock salt superstructures

Atom	Position	x	y	z	Analogues
β-Li_2SnO_3: *C2/c* ($Z=8$), $a=5.295$, $b=9.184$, $c=10.032$ Å, $\beta=100.13°$					
Li1	8f	0.239	0.078	−0.001	Li_3ReO_4
Li2	4d	1/4	1/4	1/2	
Li3	4e	0	0.083	1/4	
Sn1	4e	0	0.4165	1/4	
Sn2	4e	0	0.7508	1/4	
O1	8f	0.1337	0.2597	0.1333	
O2	8f	0.1102	0.5844	0.1342	
O3	8f	0.1346	0.9092	0.1329	
Li_2ZrO_3: *Cc* ($Z=4$), $a=5.427$, $b=9.025$, $c=5.427$ Å, $\beta=112.75°$					
Li1	4a	0	0.420	0	None known
Li2	4a	0	0.750	0	
Zr	4a	0	0.0916	0	
O1	4a	0.216	0.261	0.330	
O2	4a	0.265	0.555	0.216	
O3	4a	0.216	0.908	0.250	
β-Na_2PtO_3: *Fddd* ($Z=16$), $a=18.838$, $b=6.282$, $c=9.062$ Å					
Na1	16e	0.258	0	0	None known
Na2	16e	0.579	0	0	
Pt1	16e	0.0838	0	0	
O1	32h	0.158	0.216	0.023	
O2	16f	0	0.211	0	

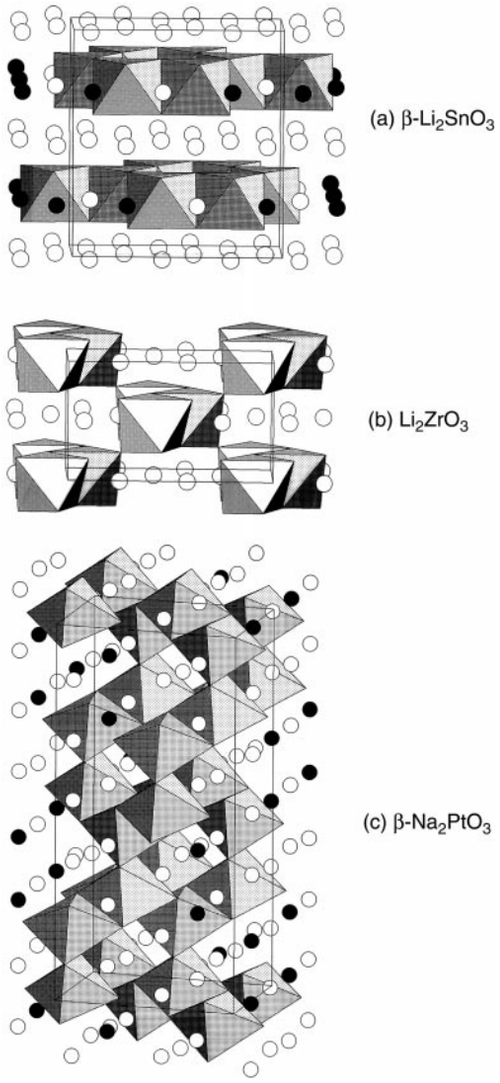

Fig. 10 Rock salt structure types of composition A_2BO_3 showing BO_6 octahedra. A cations are shown as white spheres and B cations as black spheres.

composed of the same type of octahedral environment, but the way in which the octahedra are oriented relative to each other differs.

A_5BO_6

Li_5ReO_6

The only structure to have been observed in systems which are strictly of composition A_5BO_6, is the Li_5ReO_6 structure type, adopted by phases Li_5BO_6 (B = Re, Os) and Na_5BO_6 (B = Os, I).[38,39]

Mixed cation layers of Li and Re alternate with layers of Li. The ordering of Li and Re in alternate layers is shown in Fig. 12(a); it is similar to that of Li and Sn in alternate layers of β-Li_2SnO_3, if we imagine that the A and B positions are swapped. The cation layers correspond to the (0 0 2) planes of the unit cell. Crystallographic data for the A_5BO_6 rock salt superstructures are presented in Table 3.

$Li_3Ni_2TaO_6$

$Li_3Ni_2TaO_6$ has Ta ordered over one set of octahedral sites with Li and Ni partially ordered over three more octahedral sites.[40] If we consider that the Li and Ni occupancy is statistical, the $Li_3Ni_2TaO_6$ structure is a second example of an A_5BO_6 superstructure. Each cation layer is mixed and adopts

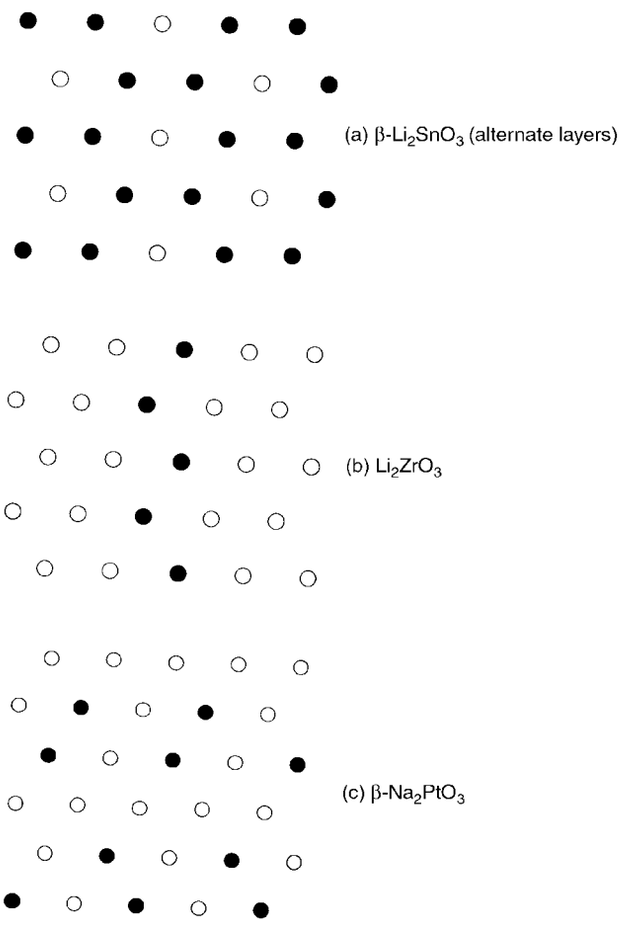

Fig. 11 Cation ordering patterns adopted between cp oxygen layers in A_2BO_3 rock salt phases. A cations are shown as white spheres and B cations as black spheres.

the ordering pattern shown in Fig. 12(b). A six-layer repeat sequence corresponding to the (0 2 6) planes in the unit cell is observed and, as in β-Na_2PtO_3, subsequent cation layers are

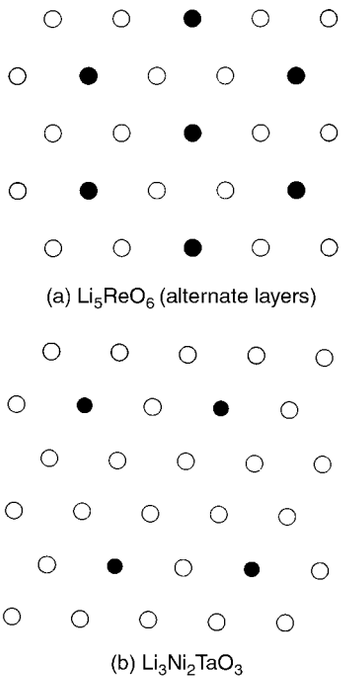

Fig. 12 Cation ordering patterns adopted between cp oxygen layers in A_5BO_6 rock salt phases. A cations are shown as white spheres and B cations as black spheres.

Table 3 Crystallographic data for A_5BO_6 rock salt superstructures

Atom	Position	x	y	z	Analogues
Li_5ReO_6: *C2/m* ($Z=2$), $a=5.0679$, $b=8.7315$, $c=5.0293$ Å, $\beta=110.24°$					
Li1	4g	0	0.6686	0	Li_5BO_6 (Re, Os), Na_5BO_6 (Os, In), *cf.* $Li_3Zn_2SbO_6$, $Li_3Zn_2BiO_6$
Li2	2d	0	1/2	1/2	
Li3	4h	1/2	0.3338	1/2	
Re	2a	0	0	0	
O1	8j	0.2706	0.3478	0.7639	
O2	4i	0.2756	1/2	0.2277	
$Li_3Ni_2TaO_6$: *Fddd* ($Z=8$), $a=8.4259$, $b=5.9073$, $c=17.7329$ Å					
Ta1	8a	1/8	1/8	1/8	$Li_3Ni_2NbO_6$, $Li_3Ni_2SbO_6$, $Li_3Mg_2NbO_6$, $Li_3Co_2TaO_6$, $Li_3Co_2NbO_6$
Li1/Ni1	16g	1/8	1/8	0.2928	
Li2/Ni2	16g	1/8	5/8	0.2864	
Li3/Ni3	8b	1/8	5/8	1/8	
O1	16f	1/8	0.357	1/8	
O2	32h	0.110	0.378	0.2969	

staggered. However, in β-Na_2PtO_3, a row of Na alternates with two rows of mixed cations, whereas in $Li_3Ni_2TaO_6$, there are two rows of Li and one of mixed cations between cp oxygen layers. Other phases, $Li_3M_2XO_6$ ($M_2X=Ni_2Nb$, Co_2Ta and Mg_2Nb), form a similar rock salt superstructure;[41] the partial order of the Li and M sites varies for different cation combinations.

$Li_3Zn_2SbO_6$

$Li_3Zn_2MO_6$ (M = Bi, Sb) has a rock salt superstructure[42] in which all three cations are completely ordered. Although, therefore, $Li_3Zn_2MO_6$ cannot be considered as strictly of type A_5BO_6 since there are three crystallographically distinct cation species, it is worth contrasting with $Li_3Ni_2TaO_6$ because of their compositional similarity. Within the cp oxygen layers, nets of Li alternate with nets of Zn and Sb which are ordered in a manner equivalent to the ordering of Li and Re in Li_5ReO_6 [Fig. 12(a)]. Zn and Sb lie in the (0 0 2) plane of the monoclinic unit cell.

Comparison of A_5BO_6 structure types

For A_5BO_6 compositions, the only coordination environment in which the electrovalency of oxygen is balanced is OA_5B. There are no octahedra in which two B cations are present; the BO_6 octahedra are, thus, isolated from each other. The BO_6 octahedra are oriented differently in Li_5ReO_6 and $Li_3Ni_2TaO_6$. In an analogous manner to the ABO_2 and A_2BO_3 systems, the reason for this type of A–B order would appear to be either the polarisation energy gained by aligning the B cations into layers (Li_5ReO_6 structure) or the energy associated with maximising the B–B cation distance ($Li_3Ni_2TaO_6$ structure).

Other derivative rock salt structures

As mentioned in the introduction, not all rock salt superstructures fall into the three broad categories (ABO_2, A_2BO_3 and A_5BO_6) in which Pauling's rule of electrovalence is satisfied. In this section, we describe structures which do not conform to Pauling's rule, either because of the presence of a Jahn–Teller active cation or a highly charged cation which induces significant covalent character between the metal–oxygen bonds or because the A : B cation ratio does not permit electroneutrality around any oxygen. Crystallographic data for these phases are given in Table 4.

β-$NaMnO_2$

The low-temperature form of $NaMnO_2$ is a monoclinic distortion of the α-$NaFeO_2$ structure in which Mn forms four short and two long bonds. β-$NaMnO_2$, however, is orthorhombic [Fig. 13(a)][43] and the octahedral distortion is alleviated in comparison with the α polymorph. The cation order adopted by Na and Mn between cp oxygen layers is shown in Fig. 13(b). Na and Mn order in double rows of like cations; these rows are staggered between consecutive layers in a zigzag formation. Two types of cation coordination environment are displayed around oxygen, with nearest neighbours 4Na/2Mn and 2Na/4Mn, respectively.

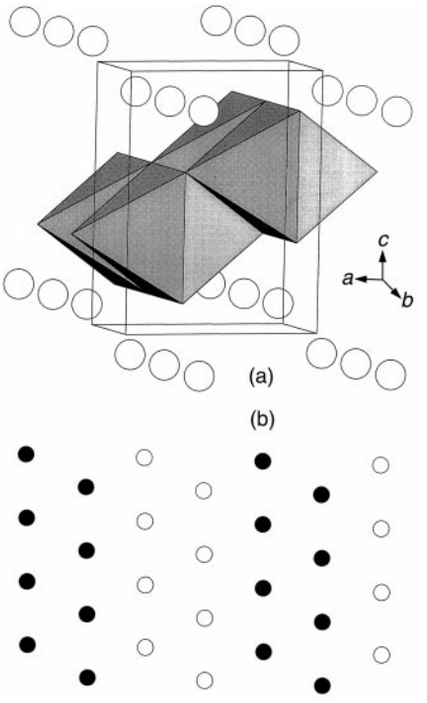

Fig. 13 (a) Crystal structure of β-$NaMnO_2$ showing MnO_6 octahedra; Na atoms are shown as white circles. (b) Cation order adopted by Na (white circles) and Mn (black circles) between cp oxygen layers.

Na_3BiO_4

A small number of phases of composition A_3BO_4 form structures analogous to Na_3BiO_4[44] [Fig. 14(a)]. The BiO_6 octahedra edge-share in zigzag chains in every second cation layer between cp oxygens; every other cation layer is fully occupied by Na. The cation ordering pattern adopted by Na and Bi is shown in Fig. 14(b), in which the zigzag Bi and Na chains are clearly visible. Recently, the crystal structure of Li_3SbO_4 was confirmed to be analogous to Na_3BiO_4 by the Rietveld method from X-ray powder diffraction data.[45]

Table 4 Crystallographic data for other rock salt superstructure phases.

Atom	Position	x	y	z	Analogues
β-$NaMnO_2$: *Pmmn* ($Z=2$), $a=4.77$, $b=2.852$, $c=6.31$ Å					
Na	4f	1/4	1/4	1/2	None known
Mn	4b	0	1/2	1/4	
O1	4e	1/4	1/4	0	
O2	4d	0	0	1/4	
Na_3BiO_4: *P2/a* ($Z=2$), $a=5.79$, $b=6.59$, $c=5.41$ Å, $\beta=109.4°$					
Na1	2e	0	0.619	1/4	Li_3SbO_4, Li_3RuO_4
Na2	2f	1/2	0.874	1/4	
Na3	2f	1/2	0.394	1/4	
Bi	2e	0	0.136	1/4	
O1	4g	0.203	0.103	0	
O2	4g	0.232	0.342	0.471	
Li_3NbO_4: $I\bar{4}3m$ ($Z=8$), $a=8.412$ Å					
Li	24g	0.3782	0.3782	0.1046	None known
Nb	8c	0.1403	0.1403	0.1403	
O1	8c	0.8910	0.8910	0.8910	
O2	24g	0.1247	0.1247	0.3601	
α-Li_3TaO_4: *P2* ($Z=6$), $a=6.027$, $b=6.004$, $c=12.822$ Å, $\beta=103.60°$					
Ta1	1c	0.5	0	0	None known
Ta2	2e	0.867	0.186	0.169	
Ta3	2e	0.636	0.450	0.332	
Ta4	1b	0	0.736	0.5	
Li11	1a	0	0.532	0	
Li12	2e	0.340	0.747	0.165	
Li13	1d	0.209	−0.023	0.349	
Li14	1a	0.5	0.233	0.5	
Li21	2e	0	−0.008	0	
Li22	1d	0.332	0.220	0.141	
Li23	1c	0.163	0.476	0.336	
Li24	2e	0.5	0.741	0.5	
Li31	1b	0.5	0.448	0	
Li32	2e	0.847	0.720	0.163	
Li33	2e	0.629	−0.047	0.332	
Li34	1b	0	0.182	0.5	
O1	2e	0.262	0.206	−0.013	
O2	2e	0.268	0.726	0.006	
O3	2e	0.075	−0.018	0.170	
O4	2e	0.590	−0.019	0.157	
O5	2e	0.066	0.452	0.158	
O6	2e	0.598	0.446	0.179	
O7	2e	0.439	0.216	0.335	
O8	2e	0.902	0.219	0.327	
O9	2e	0.426	0.690	0.328	
O10	2e	0.902	0.693	0.340	
O11	2e	0.235	−0.038	0.493	
O12	2e	0.235	0.489	0.507	
γ-Li_2CuZrO_4: *Cccm* ($Z=4$), $a=9.4013$, $b=5.8951$, $c=5.8635$ Å					
Li1	4f	1/4	1/4	1/2	None known
Li2	4b	0	1/2	1/4	
Zr1	4e	1/4	1/4	0	
Cu1	4d	0	0	1/4	
O1	8l	−0.030	0.239	1/2	
O2	8g	0.265	0	1/4	
β-Li_2CuZrO_4: *I4m2* ($Z=2$), $a=4.1618$, $c=9.4157$ Å					
Li1	2a	0	0	0	None known
Cu	2b	0	0	1/2	
Zr	2c	0	1/2	1/4	
Li2	2d	0	1/2	3/4	
O1	4e	0	0	0.233	
O2	4f	0	1/2	0.468	
Li_4UO_5: *I4/m* ($Z=2$), $a=6.736$, $c=4.457$ Å					
Li	8h	0.28	0.097	0	Na_4UO_5, Li_4NpO_5
U	2a	0	0	0	
O1	2b	0	0	1/2	
O2	8h	0.197	0.383	0	

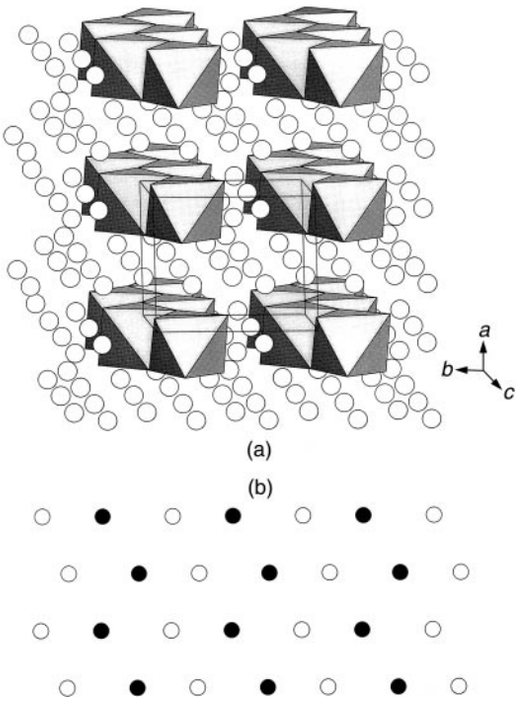

Fig. 14 (a) Crystal structure of Na_3BiO_4 showing BiO_6 octahedra; Na atoms are shown as white circles. (b) Cation order adopted by Na (white circles) and Bi (black circles) between cp oxygen layers.

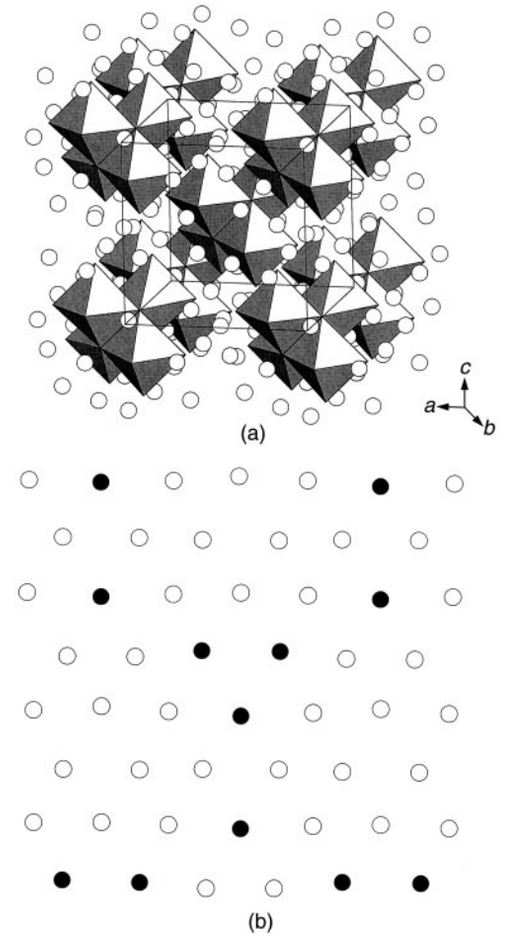

Fig. 15 (a) Crystal structure of Li_3NbO_4 showing Nb_4O_{16} clusters; Li atoms are shown as white circles. (b) One type of cation order adopted by Li (white circles) and Nb (black circles) between cp oxygen layers.

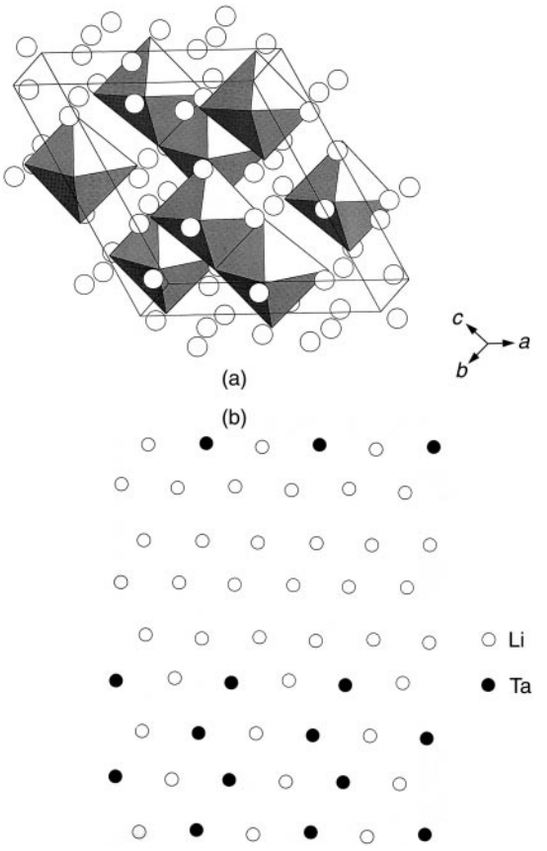

Fig. 16 (a) Crystal structure of β-Li_3TaO_4 showing TaO_6 octahedra; Li atoms are shown as white circles. (b) Cation order adopted by Li (white circles) and Ta (black circles) between cp oxygen layers in β-Li_3TaO_4.

Li_3RuO_4 has also been shown to be isostructural with Na_3BiO_4; in this case, the crystal structure was determined by energy minimisation procedures.[46]

Li_3NbO_4

The crystal structure of Li_3NbO_4 was recently verified with a single crystal obtained from a LiCl flux.[47,48] Fig. 15(a) shows the Li_3NbO_4 structure in which the most striking feature is the presence of Nb_4O_{16} clusters which form a body-centred cubic lattice. Fig. 15(b) shows a layer of Li and Nb cations lying between cp oxygens in which three niobiums in the centre of the diagram form an Nb_4O_{16} tetramer with a niobium in the subsequent layer.

β-Li_3TaO_4

Lithium orthotantalate, Li_3TaO_4, exists in three polymorphic forms: a low-temperature β phase, a high-temperature α phase and an intermediate-temperature modification which is considered to be disordered.[49,50] The structure of the monoclinic β phase, shown in Fig. 16(a), consists of edge-sharing TaO_6 octahedra which form a series of zigzag chains. The structure can also be understood in terms of layer packing of the cations between cp oxygens (Fig. 16(b)): cation blocks of four rows of Li and Ta are separated by blocks of four rows of only Li; subsequent cation layers are staggered such that like blocks run in a step-wise fashion.

α-Li_3TaO_4

The high-temperature α phase is related to the β polymorph by means of an intricate series of shifts of the Ta cations resulting in a lowering of the monoclinic symmetry from *C*2/*c* in the β phase to *P*2. The structure [Fig. 17(a)] is again composed of zigzag chains of TaO_6 octahedra but the configuration of the

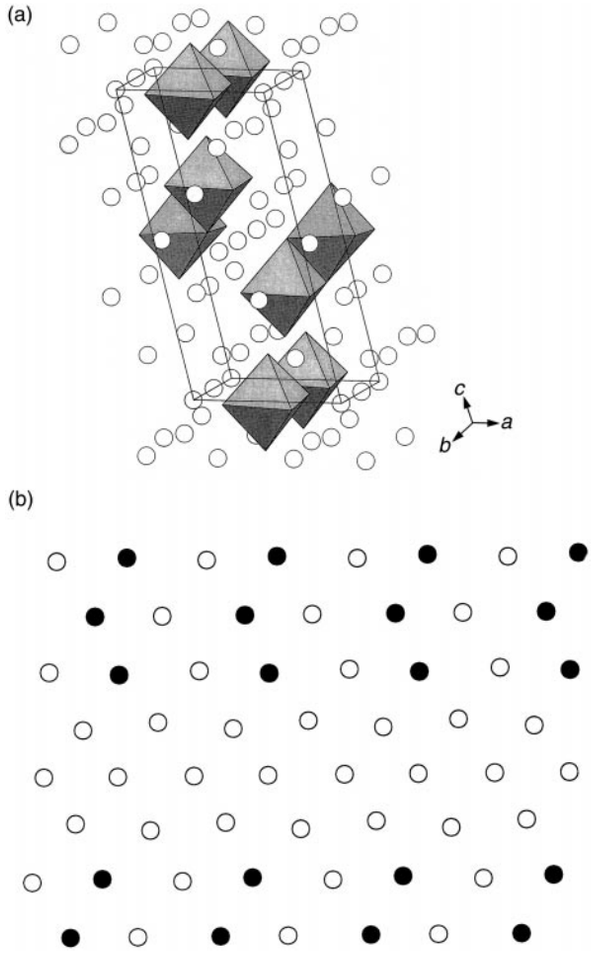

Fig. 17 (a) Crystal structure of α-Li_3TaO_4 showing TaO_6 octahedra; Li atoms are shown as white circles. (b) Cation order adopted by Li (white circles) and Ta (black circles) between close-packed oxygen layers in α-Li_3TaO_4.

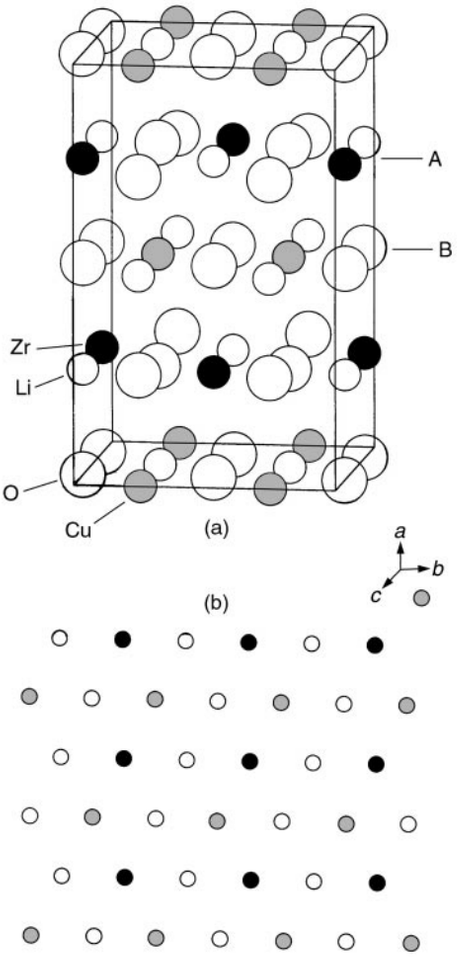

Fig. 18 (a) Crystal structure of γ-Li_2CuZrO_4 showing Li–Zr layers (A) and Li–Cu layers (B) (A and B layers are not close-packed). (b) Cation order adopted by Li (white circles), Cu (shaded circles) and Zr (black circles) between cp oxygen layers in γ-Li_2CuZrO_4.

chains is different from the β phase.§ In terms of cation order between cp layers, the relationship between the two polymorphs is readily seen. Whereas in β-Li_3TaO_4, the blocks of Li and Ta extend to four cation rows and are separated by blocks of four rows of Li, in the α polymorph, both mixed-cation and Li blocks are composed of only three cation rows [Fig. 17(b)].

γ-Li_2CuZrO_4

Li_2CuZrO_4 exhibits high- and low-temperature ordered forms.[51] Low-temperature γ-Li_2CuZrO_4 unusually shows complete cation order amongst the three different cation types. Fig. 18(a) shows the structure of γ-Li_2CuZrO_4 in which layers, but not cp layers, of Li and Zr (labelled A) alternate with layers of Li and Cu (labelled B). Chains of CuO_6 octahedra and chains of LiO_6 octahedra are formed and run parallel to each other within the B layers. The order adopted amongst the Li, Cu and Zr cations between cp oxygen layers is shown in Fig. 18(b).

β-Li_2CuZrO_4

β-Li_2CuZrO_4 is formed from the γ polymorph by firing at 1150 °C under an O_2 flow and rapidly quenching to room temperature. In comparison to the γ phase, the Li and Cu exchange sites such that the CuO_6 octahedra no longer edge-share, but corner-share; the order between Li and Cu is, however, only partial.[52] The structure of β-Li_2CuZrO_4 is shown in Fig. 19(a); here, for clarity, the order between Li and Cu is considered as complete. The β polymorph adopts a $\sqrt{2}$ relationship with the unit cell of the α phase. We can see the relationship between the β and γ polymorphs by contrasting the order of the cations between cp layers [Fig. 18(b) and 19(b)]: swapping Li and Cu positions in every second Li–Cu row leads to an interchange of polymorphs. γ-Li_2CuZrO_4 is isostructural with γ-$LiFeO_2$ if we imagine that Cu and Zr disorder [*cf.* Fig. 3 and 19(b)].

In both β and γ structures, Cu shows a considerable Jahn–Teller elongation of its octahedra; the *c*-axis is elongated by 13% in comparison to the *c*-parameter in the γ-$LiFeO_2$ structure.

Li_4UO_5

The structure of Li_4UO_5, shown in Fig. 20(a), is built up of parallel corner-sharing UO_6 octahedra running along the *c*-direction of the tetragonal unit cell.[53] There is a distortion of the UO_6 octahedra along this direction, such that the U–O bonds are stronger in the *ab* plane. The cation order adopted by Li and U between cp oxygens is shown in Fig. 20(b). Na_4UO_5 is isostructural with Li_4UO_5.

Remarks on other derivative rock salt structures

In the case of rock salt phases satisfying Pauling's rule of electroneutrality, the type of structure which forms is

§For a more detailed explanation of the configuration of the chains of TaO_6 octahedra in α- and β-Li_3TaO_4, the interested reader is referred to ref. 50.

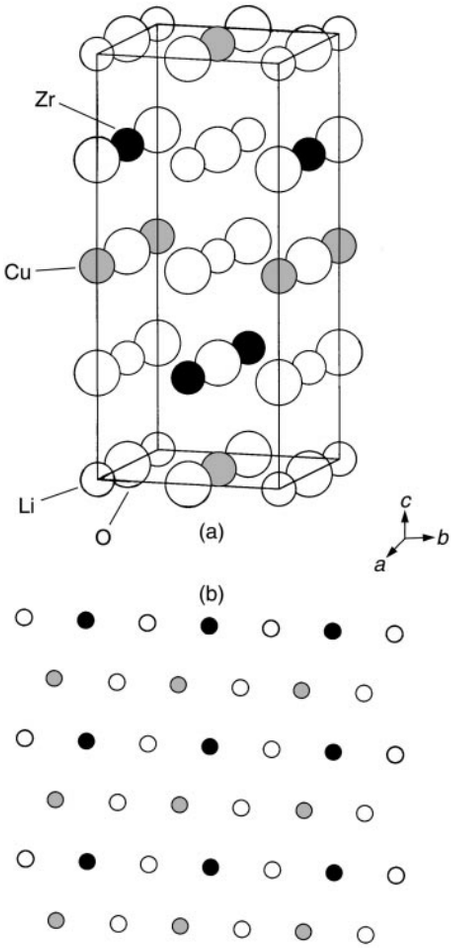

Fig. 19 (a) Crystal structure of β-Li_2CuZrO_4. (b) Cation order adopted by Li (white circles), Cu (shaded circles) and Zr (black circles) between cp oxygen layers in β-Li_2CuZrO_4.

influenced by the polarization energy of the anions and the B–B Coulombic repulsion energy; whichever term is more dominant appears to be a function of the B to A cation radius ratio. We have encountered three phases, β-$NaMnO_2$ and the β and γ polymorphs of Li_2CuZrO_4, in which the energy associated with a Jahn–Teller distortion of the transition-metal environment is another consideration which dictates the type of structure formation. In these cases, the MO_6 octahedra of the Jahn–Teller active cations prefer to be aligned such that the distortion is macroscopic throughout the crystal. For rock salt phases of general composition A_3BO_4 and A_4BO_5, the principles for choice of structure formation appear to be more complex. This difficulty is highlighted in the cases of Li_3NbO_4, α- and β-Li_3TaO_4 and Li_3SbO_4 which form markedly different types of rock salt superstructure despite their normally similar crystallochemical behaviour, similar pentavalent-cation radii[54] and M(v)–O bond lengths.[4] As in simpler cases, the lattice energies of these structure types must be a balance of the Madelung potential of the cation arrangement and the degree of partial covalency associated with the M–O bonds. The energy differences between the stability fields of the different crystal structures may be so small, however, that the degree of partial covalency in the M–O bond and, in turn, the electronegativity of the highly charged cation are critical elements in the choice of structure which is adopted.

As an addendum, we should inform the reader that we have omitted a number of A_3BO_4 and A_4BO_5 compositions with rock salt superstructures from this review. With the exception of genuine oversights, these compositions fall into two categories: phases such as Li_4WO_5[55] and Li_4MoO_5 whose

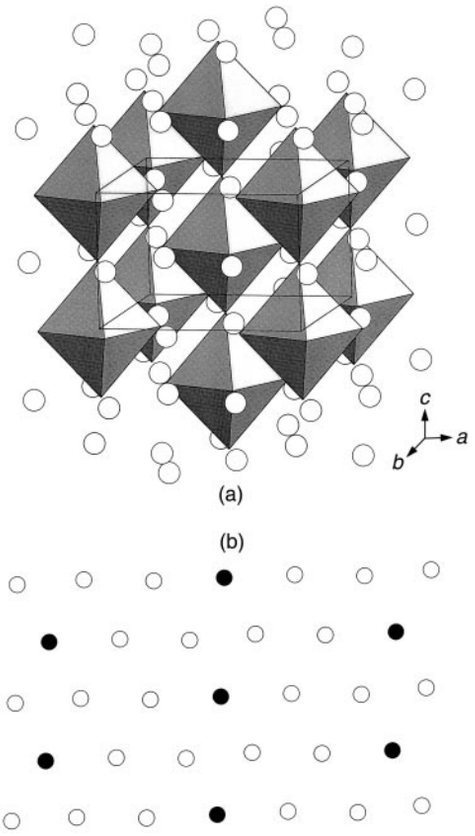

Fig. 20 (a) Crystal structure of Li_4UO_5 showing UO_6 octahedra; Li atoms are shown as white circles. (b) Cation order adopted by Li (white circles) and U (black circles) between cp oxygens.

cations show only short-range order and those phases, including Li_3BiO_4 and Li_3UO_4, in which the Li positions have not yet been conclusively determined due to the resolution of their structure from early X-ray powder diffraction work.[49]

Summary

Rock salt superstructures arise in complex systems with more than one type of cation as a result of the non-statistical manner in which the cation sites in the NaCl structure type are occupied. This is most likely to occur when two cations (A and B) with different charges are present.

In rock salt phases which satisfy Pauling's rule of electroneutrality, only three A, B combinations are observed: ABO_2, A_2BO_3 and A_5BO_6, where A is monovalent. In ABO_2 and A_2BO_3 systems, the cations may be arranged in two types of ordered environment around oxygen. The observed structure types are formed from the edge-sharing of these octahedra in the three crystallographic directions. The structure types may differ by the type of octahedra adopted and/or their relative orientation. In A_5BO_6 systems, the cations can be arranged in only one type of environment around oxygen. Different A_5BO_6 structures are formed when the octahedra adopt different relative orientations. When Pauling's rule of electroneutrality is not observed, as in A_3BO_4 and A_4BO_5 systems, structure types tend to be more complex. The octahedral cation environment of oxygen may be better considered in terms of the bond valence approach since the *local* environment of oxygen is not strictly electroneutral, in terms of Pauling's definition. More than one type of octahedral cation environment is observed and these octahedra are more obviously distorted with greater covalent character in the bonds than found in the classically 'ionic' NaCl structure. In general, the greater complexity of these structure types means that they are most easily

considered, and contrasted with simpler parent structures, in terms of the cation order adopted in the layers between cp oxygens.

The choice of structure formed for a given composition may be simplified as being dependent on the greater of two energy terms which affect the crystal lattice energy: the polarisation energy of the anions and the energy associated with the B–B Coulombic repulsion energy. The highly charged B cations tend to polarise the anions to a greater extent when they are small and are, consequently, aligned in layers. In more ionic crystals with larger B cations, the repulsion energy between B cations is a greater consideration and is minimized by maximizing the B–B cation distance; layered structures then become less likely. Whereas in the ABO_2, A_2BO_3 and A_5BO_6 structures, the most important of these influences is often readily apparent by inspection of the crystal structure, in A_3BO_4 and A_5BO_6 systems, the structure which forms is usually a compromise between these two opposing factors.

References

1 M. O'Keeffe, *Acta Crystallogr., Sect. A*, 1977, **33**, 924.
2 M. O'Keeffe and B. G. Hyde, *J. Solid State Chem.*, 1982, **44**, 24.
3 A. F. Wells, *Structural Inorganic Chemistry*, 5th edn., Oxford Science Publications, Oxford, 1984, pp. 238–245.
4 A. R. West, *Solid State Chemistry and its Applications*, 1st edn., Wiley, Chichester, 1984.
5 G. Donnay and J. D. H. Donnay, *Acta Crystallogr., Sect. B*, 1973, **29**, 1417.
6 I. D. Brown and R. D. Shannon, *Acta Crystallogr., Sect. A*, 1973, **29**, 266.
7 R. Allmann, *Mh. Chem.*, 1975, **106**, 779.
8 I. D. Brown, *Chem. Soc. Rev.*, 1978, **7**, 359.
9 I. D. Brown, in *Structure and Bonding in Crystals*, 1st edn., ed. M. O'Keeffe and A. Navrotsky, Academic Press, London, 1981, vol. 2, pp. 1–29.
10 J. C. Anderson and M. Schreiber, *J. Phys. Chem. Solids*, 1969, **25**, 961.
11 R. W. G. Wyckoff, *Crystal Structures*, 2nd edn., Interscience, New York, 1964, vol. 2, p. 312.
12 Y. B. Kuo, W. Scheld and R. Hoppe, *Z. Kristallogr.*, 1983, **164**, 121.
13 M. Marezio and J. P. Remeika, *J. Chem. Phys.*, 1966, **44**, 3348.
14 M. Castellanos, M. Chavez Martinez and A. R. West, *Z. Kristallogr.*, 1990, **190**, 161.
15 H. A. Graf and H. Schäfer, *Z. Anorg. Allg. Chem.*, 1975, **414**, 211.
16 R. Famery, P. Bassoul and F. Queyroux, *J. Solid State Chem.*, 1965, **57**, 178.
17 J. C. Anderson, S. K. Dey and V. Halpern, *J. Phys. Chem. Solids*, 1968, **29**, 163.
18 M. Brunel and F. de Bergevin, *J. Phys. Chem. Solids*, 1968, **29**, 163.
19 F. de Bergevin and M. Brunel, *Bull. Soc. Fr. Mineral. Cristallogr.*, 1968, **91**, 621.
20 M. Brunel and F. de Bergevin, *J. Phys. Chem. Solids*, 1969, **30**, 2011.
21 M. Brunel and F. de Bergevin, *C. R. Acad. Sci., Ser. B*, 1970, **270**, 1030.
22 R. Hoppe and B. Schepers, *Z. Anorg. Allg. Chem.*, 1958, **295**, 233.
23 T. A. Hewston and B. L Chamberland, *J. Phys. Chem. Solids*, 1987, **48**, 97 and references therein.
24 A. R Armstrong and P. G. Bruce, *Nature*, 1996, **381**, 499.
25 L. D. Dyer, B. S. Dorie and G. P. Smith, *J. Am. Chem. Soc.*, 1954, **76**, 1499.
26 P. F. Bongers, PhD Thesis, University of Leiden, The Netherlands, 1957.
27 A. Lecerf, *Ann. Chim. (Paris)*, 1962, **7**, 513.
28 A. Deschanvres, B. Raveau and Z. Sekkal, *Mater. Res. Bull.*, 1971, **6**, 699.
29 D. W. Murphy, M. Greenblatt, S. Zahurak, R. J. Cava, J. V. Waszczak, G. W. Hull and R. S. Hutton, *Rev. Chim. Miner.*, 1982, **19**, 441.
30 R. J. Cava, D. W. Murphy, S. Zahurak, A. Santoro and R. S. Roth, *J. Solid State Chem.*, 1984, **53**, 64.
31 M. Brunel, F. de Bergevin and M. Gondrand, *J. Phys. Chem. Solids*, 1972, **33**, 1927.
32 J. Hauck, *Acta Crystallogr., Sect. A*, 1980, **36**, 228.
33 J. F. Dorrian and R. E. Newnham, *Mater. Res. Bull.*, 1969, **4**, 179.
34 G. Von Kreuzberg, F. Stewner and R. Hoppe, *Z. Anorg. Allg. Chem.*, 1970, **379**, 242.
35 P. Quintana, J. Leal, R. A. Howie and A. R. West, *Mater. Res. Bull.*, 1989, **24**, 1385.
36 G. Dittrich and R. Hoppe, *Z. Anorg. Allg. Chem.*, 1984, **512**, 19.
37 Von. W. Urland and R. Hoppe, *Z. Anorg. Allg. Chem.*, 1972, **392**, 23.
38 T. Betz and R. Hoppe, *Z. Anorg. Allg. Chem.*, 1984, **512**, 19.
39 T. Betz and R. Hoppe, *Z. Anorg. Allg. Chem.*, 1985, **524**, 17.
40 J. G. Fletcher, G. C. Mather, A. R. West, M. Castellanos and M. P Gutierrez, *J. Mater. Chem.*, 1994, **4**, 1305.
41 G. C. Mather, R. I. Smith, J. M. S. Skakle, J. G. Fletcher, M. A. Castellanos, M. P. Gutierrez and A. R. West, *J. Mater. Chem.*, 1995, **5**(8), 1177.
42 C. Greaves and S. M. A. Katib, *Mater. Res. Bull.*, 1990, **25**, 175.
43 J. P. Parant, R. Olazawaga, M. Devalette, C. Fouassier and P. Hagenmuller, *J. Solid State Chem.*, 1971, **3**, 1.
44 B. Schwedes and R. Hoppe, *Z. Anorg. Allg. Chem.*, 1972, **393**, 136.
45 J. M. S. Skakle, M. A. Castellanos, S. T. Tovar, S. M. Fray and A. R. West, *J. Mater. Chem.*, 1996, **6**, 1939.
46 T. Bush, C. R. A. Catlow and P. D. Battle, *J. Mater. Chem.*, 1995, **5**, 1269.
47 K. Ukei, H. Suzuki, T. Shishido and T. Fukuda, *Acta Crystallogr., Sect. C*, 1994, **50**, 655.
48 G. Blasse, *Z. Anorg. Allg. Chem.*, 1963, **326**, 44.
49 G. Blasse, *Z. Anorg. Allg. Chem.*, 1964, **331**, 44.
50 M. Zocchi, M. Gatti, A. Santoro and R. S. Roth, *J. Solid State Chem.*, 1983, **48**, 420.
51 G. C. Mather, PhD Thesis, University of Aberdeen, Scotland, 1995.
52 C. Dussarrat, G. C. Mather, V. Caignaert, B. Domengès, J. G. Fletcher and A. R. West, unpublished results.
53 H. Hoekstra and S. Siegel, *J. Inorg. Nucl. Chem.*, 1964, **26**, 693.
54 R. D. Shannon and C. T. Prewitt, *Acta Crystallogr., Sect. B*, 1969, **25**, 925.
55 B. Reau, *Bull. Soc. Chim. Fr.*, 1967, 3873.